JOURNAL OF MATERIALS SCIENCE 12 (1977) 2519–2524

Radial cracks in boron fibres

JORGE VEGA-BOGGIO, OLOF VINGSBO
Institute of Technology, Uppsala University, Box 534, S-751 21 Uppsala, Sweden

The morphology of so-called radial cracks in boron fibres is studied in transverse and axial cross-sections, as well as in fracture surfaces. A formation mechanism is proposed in terms of the transverse residual stress pattern. Small pre-existing voids, (so-called proximate voids) are found to act as stress concentrators which contribute to the opening up of radial cracks in quantitative agreement with the Griffith criterion for brittle fracture.

1. Radial cracks and tensile failure in boron fibres

It has been verified in several investigations [1–3, 5, 6] that the fracture stress of boron fibres is strongly correlated to the type of imperfection triggering crack nucleation. The most critically weakening feature is the so-called radial crack. While well manufactured high-quality commercial fibres display tensile fracture stresses ranging from 3 to 4 kN mm^{-2}, the presence of radial cracks reduces the strength to about 0.5 to 2 kN mm^{-2}. It is thus of great interest to be able to suppress the formation of radial cracks. Nevertheless, the origin is not known and it is not even clear, whether the formation starts already during the fibre growth process or later, during handling the manufactured fibre (rolling on spools, preparation of test specimens etc.).

2. Residual stresses in boron fibres

Boron fibres are manufactured by chemical vapour deposition, as suggested by Talley *et al.* [1] in 1959. Boron trichloride and hydrogen react on a tungsten wire, 10 to 12 μm in diameter, electrically heated to about 1500 K. The unidirectional diffusion of boron into the core during the manufacturing process causes a transformation of the tungsten wire into a polycrystalline mixture of tungsten borides. This transformation results in an expansion of the original substrate during the mantle growth, giving rise to residual stresses, compressive in the core and dilational in the surrounding boron mantle. The quenching at the end of the manufacturing process implies a compressive residual stress in the outermost part of the mantle.

Measurements of the residual stresses in boron fibres have been reported in the literature. [2–4] and are summarized in the schematic residual stress pattern of Fig. 1. The radial crack extends

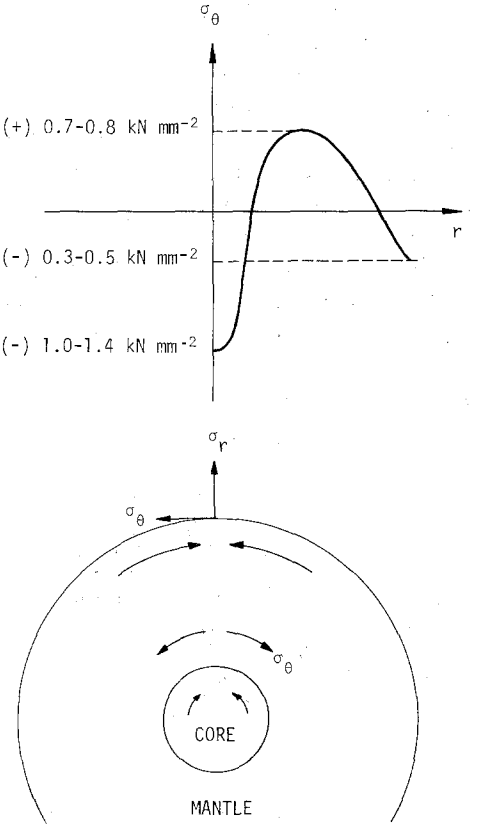

Figure 1 Schematic residual stress pattern in the cross-section of a boron fibre.

from the fibre core and outwards through the mantle, generally to the transition region between dilational and compression residual stresses. The axial extension is considerable (of the order of mm), while the tangential dimension is essentially negligible.

The formation of radial cracks as an exclusive consequence of the residual stress situation pictured in Fig. 1, would require a critical fracture stress of the order of 0.8 $kN\,mm^{-2}$, corresponding to the dilational stress peak. Compared to the measured fracture stresses, however, this value is too low to create a crack in a flawless boron mantle. Consequently, residual stresses cannot be the only origin of radial cracks.

In the present work, which is one of a series of investigations on fracture properties of boron fibres, the morphology of radial cracks is studied and formation mechanisms investigated in terms of other imperfections, correlated to residual stresses.

3. Material and experimental

A spool of continous 100 μm fibre, laboratory produced by a commercial manufacturer, showed a high frequency of radial crack initiated fracture, and was chosen for the present study.

100 tensile test specimens of 50 mm length were cut at random from the spool and tested to failure in a Lorentzen and Wettres (Allwetron) micro-tensile testing machine. The gauge length was 25 mm. The debris were retained after fracture, washed, given a 200 Å thick gold coating by sputtering, and studied in emissive mode in a JSM-U3 scanning electron microscope, operated at 20 kV. Several additional specimens of 50 mm length were cut at random from the spool, and given an electrolytical coating of nickel. The resulting composite was mechanically polished, ion-etched and studied in transverse and longitudinal sections in a Reichert MeF2 light microscope as well as a JEM 200 B scanning transmission electron microscope, operated in emissive mode at 200 kV.

4. The morphology of radial cracks

Micrographs of etched transverse fibre sections may show as much as four separate radial cracks, always of the previously reported radial extension, from within the core to just inside the external mantle surface. Image examples are given in Fig. 2. It was also possible to follow the axial extension as demonstrated by Fig. 3.

The influence of residual stresses on the path of the radial cracks is quite obvious. A comparison between Figs. 1 and 2 shows that the outer crack edge roughly coincides with the outer transition between dilational and compressive stresses. Close inspection of Fig. 2a and b also shows that in both cases one of the cracks deviates from the radial direction and follows the circular transition region inside the core (at A), while the others are stopped at depths, corresponding to higher compressive stresses. Another example is given by Fig. 4, where part of the core is separated by this mechanism under the interaction of two radial cracks.

Examples were also found of the existence of another type of imperfection, the so-called proximate void [9], in the radial crack at the core-mantle interface. An image example is shown in Fig. 5.

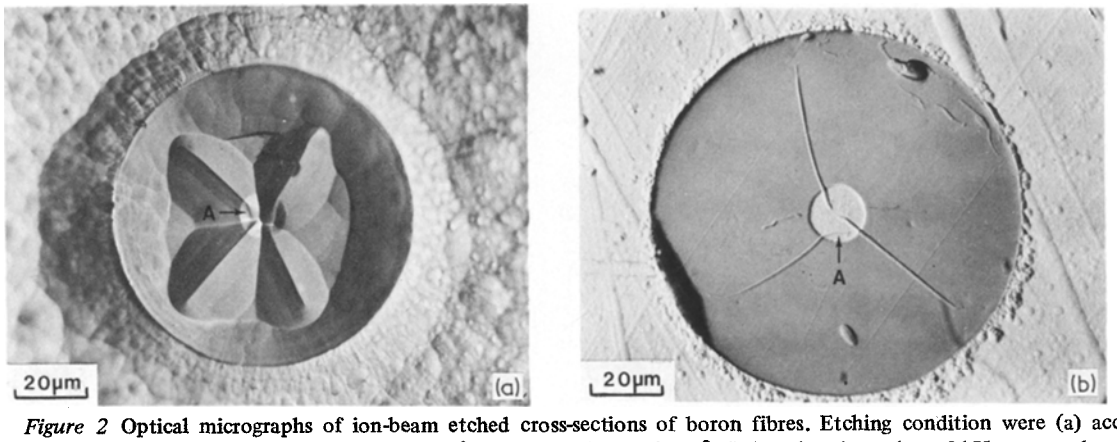

Figure 2 Optical micrographs of ion-beam etched cross-sections of boron fibres. Etching condition were (a) accelerating voltage 6 kV, current density 11 $A\,m^{-2}$ and a glancing angle 15°, (b) accelerating voltage 8 kV, current density 13 $A\,m^{-2}$ and a glancing angle of 10°. The radial cracks are stopped by the compressive stresses and sometimes deviated from the radial propagation plane (at A).

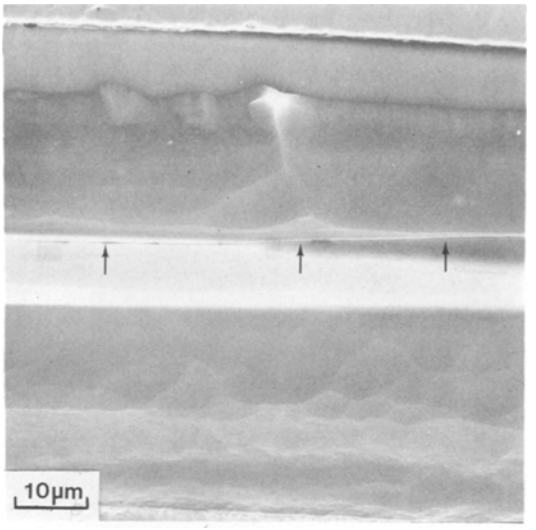

Figure 3 20 kV SEM micrograph showing an ion-beam etched axial section of a boron fibre. A radial crack is observed in the vicinity of the core–mantle interface across the whole image.

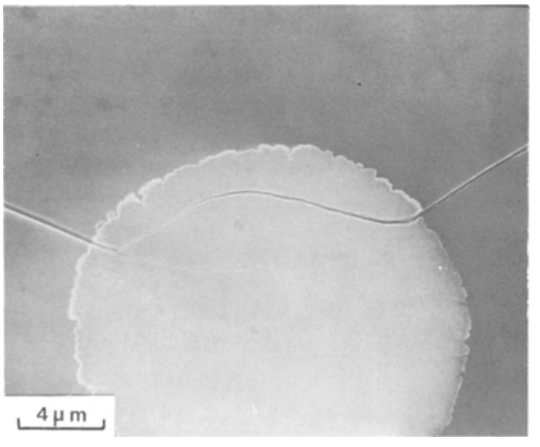

Figure 4 200 kV SEM micrograph of an ion-beam etched cross-section. Two radial cracks interact to separate part of the core.

As previously reported [6], the transverse fracture nucleation sites can generally be precisely traced by extrapolating hackle marks into the mirror zone of the fracture surface. Electron micrographs of fracture surface pairs prove that the transverse fracture is frequently nucleated at the outer edge of radial cracks, see Fig. 6. A typical feature is that the transverse crack, when propagating inwards into the fibre, follows somewhat different planes on the different sides of the radial crack. This is clearly seen in the image sequence of Fig. 6, with the corresponding topography profile schematically indicated in Fig. 6e.

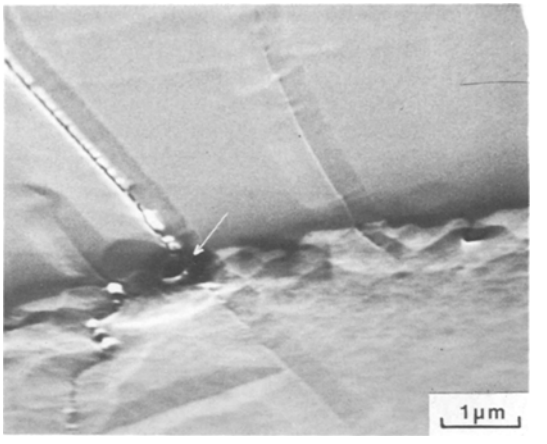

Figure 5 Proximate void (arrow) in a radial crack, at the core–mantle interface. (200 kV SEM. Ion-beam etched cross-section.)

In addition, a pair of fork-like surface steps generally extend from the radial crack edge over about 10 μm in the direction of propagation of the transverse crack, as demonstrated in Fig. 6. A few similar, but radial, surface steps are also often observed just outside the nucleation site (Fig. 6c and d). Finally, the fracture surface generally adopts the shape of a spherical cap of about 5 μm diameter around the nucleation site, as seen in Fig. 6c and d.

Occasionally, the effect of two co-operating radial cracks, of the type demonstrated in Fig. 4, is also observed in fractured fibres. Fig. 7 shows an example, from which also the location of the outer radial crack edge is clearly given.

5. The formation of radial cracks

As mentioned in Section 4, a particular type of imperfection, referred to as proximate voids, was sometimes observed at the intersection between a radial crack and the core–mantle interface. Although not frequent, this contribution in fact provides the basis of a possible formation mechanism of radial cracks. Therefore, the concept of proximate voids (PV) has to be reviewed in some detail.

In a previous work [9], the morphology of PV has been studied and a formation mechanism, active during the mantle growth in the production process, has been worked out. The completed PV has a principal shape as sketched in Fig. 8. It consists of a somewhat irregular lath-shaped void with a radial extension of up to a few μm, and often a considerably longer axial dimension. As

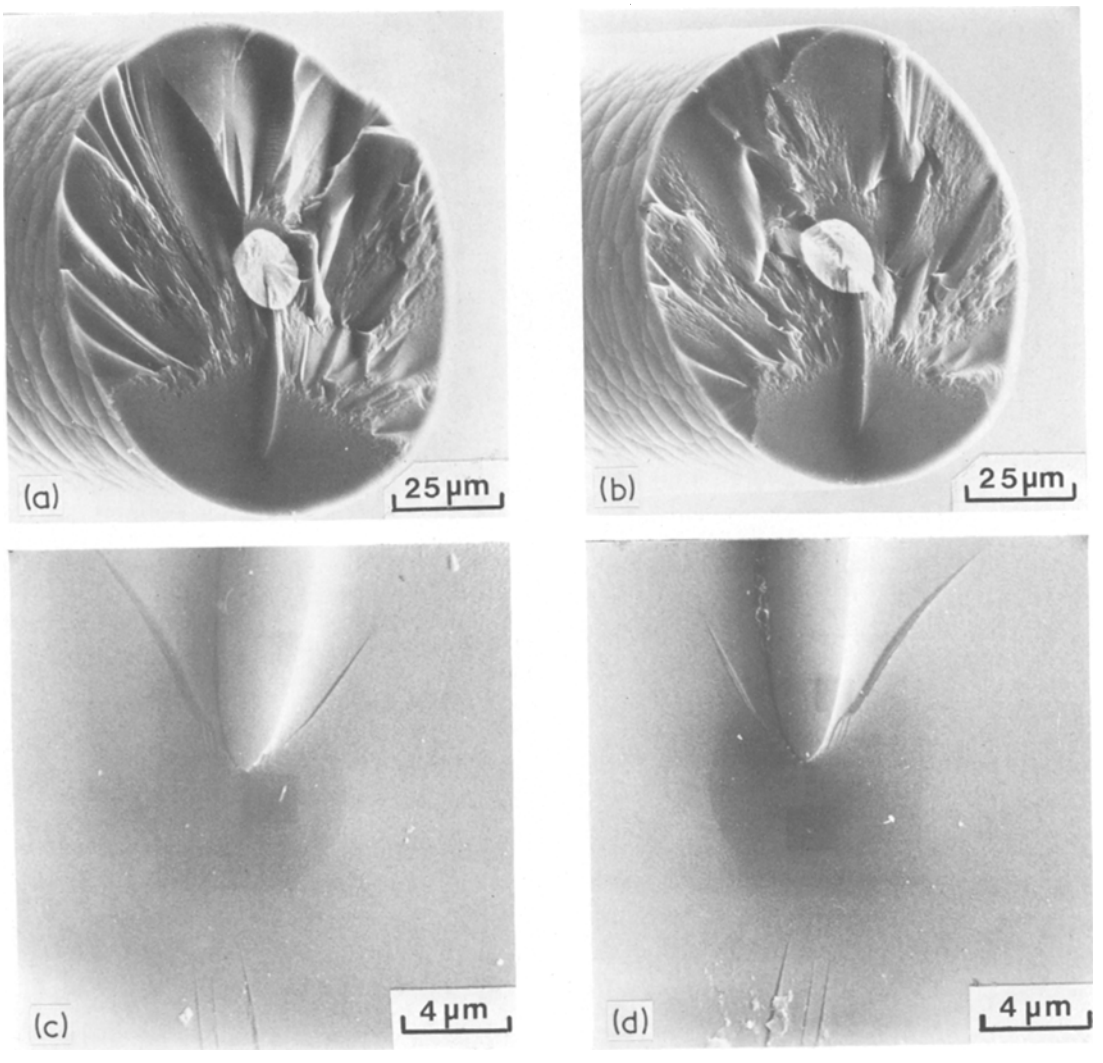

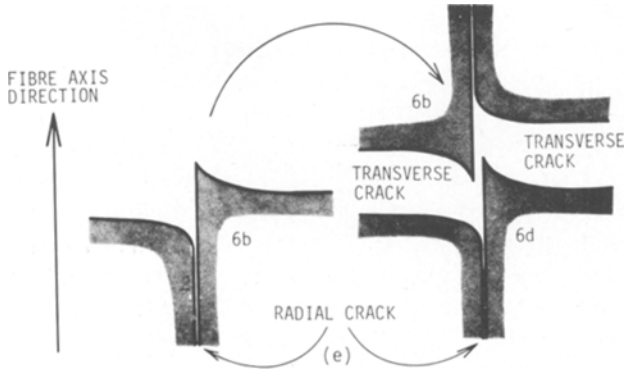

Figure 6 Fracture surface pair; (a) and (c) represent one side, (b) and (d) the opposite side, and (e) the related schematic topography profile (20 kV SEM).

previously described [7, 8], irregularities in the PV shape, for instance bulges, may act as Griffith cracks and nucleate transverse fracture. Under the influence of an externally applied axial stress σ_z in Fig. 8 the crack propagates in the r–θ plane and has an opening ellipse in the θ–z plane of major axis $2c$ in the θ direction.

The residual stresses summarized in Fig. 1, however, have a dilational, tangential component in the region just outside the core, where the PVs

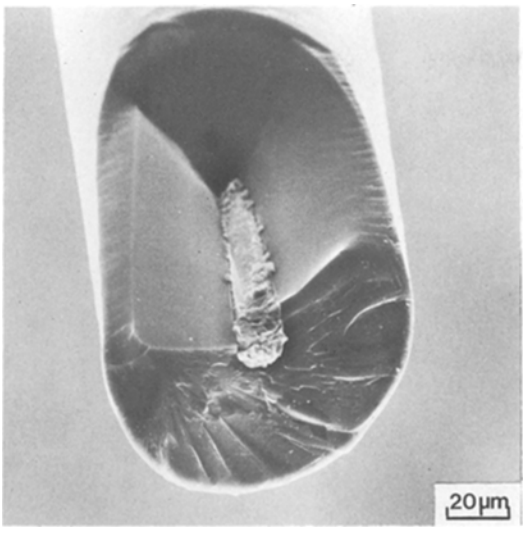

Figure 7 Two different transverse fracture surfaces, joined by radial crack surfaces. Note that the latter are of the mirror zone type (20 kV SEM).

are located, i.e. in the θ direction (σ_θ in Fig. 8). As discussed in Section 2, measured σ_θ values are not sufficient to initiate ideal cleavage along the r–z plane. If, however, Griffith's theory of fracture is applied on the geometry of Fig. 8, with σ_θ acting on the lath shaped PV as pre-existing crack nucleus, the critical void dimension is the major axis of length $2C$ in the r direction of the r–θ plane ellipse (shaded in Fig. 8). The Griffith criterion now is

$$\sigma_{rc} = \left[\frac{4E\gamma}{\pi(2C)}\right]^{1/2} \quad (1)$$

where E is Young's modulus and γ is the effective surface energy in cleavage. σ_{rc} represents the critical dilational residual stress necessary for opening up the PV in the r–z plane to a radial crack. Unlike the case of constant external load this crack does not become unstable. During the radial crack propagation, σ_θ is continously relaxed, and the crack growth proceeds at a low speed, essentially maintaining an equilibrium according to Equation 1, with a decreasing critical stress σ_{rc} matching an increasing crack length $2C$. Consequently, the character of the fracture surfaces remains of the mirror-zone type, typical of low-speed crack propagation (see Fig. 7). Eventually, the crack propagation stops, when the crack fronts reach regions of compressive residual stresses ($-\sigma_\theta$, Fig. 1).

From previous investigations [6–9] $2C$ is known to vary between 1 and 3 μm, which gives the critical stress for known E and γ [10, 8]. Table I shows the obtained variation of σ_{rc}, taking also the range of experimental γ values into account [8, 11].

These values, compared with the experimental residual stress peak of 0.8 kN mm^{-2} (Fig. 1), indicate that the mechanism suggested above is nu-

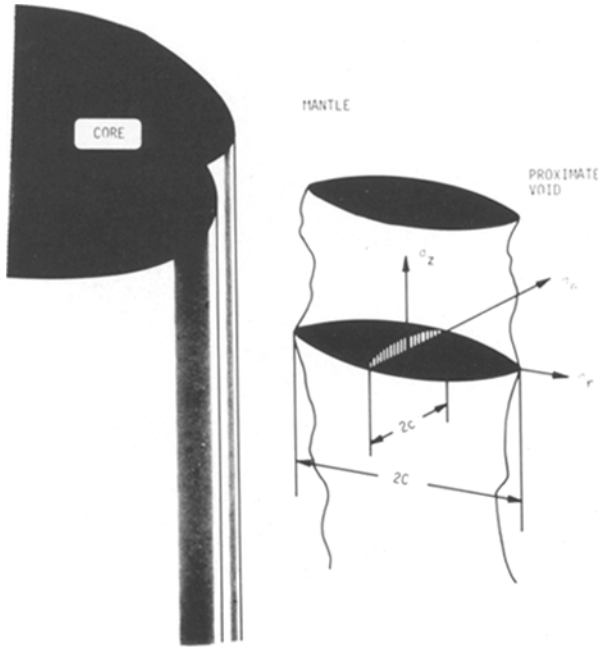

Figure 8 Schematic representation of a proximate void.

TABLE I σ_{rc} for different surface energies γ and Griffith crack lengths $2C$

γ ($J\,m^{-2}$)	$2C$ (μm)	σ_{rc} ($kN\,mm^{-2}$)
2.8	1	1.2
2.8	3	0.7
6.4	1	1.9
6.4	3	1.1

merically possible. In addition, the measurements, referred to by Fig. 1, must be expected to underestimate dilational stresses, because the probable presence of already created radial cracks will relax all tangential dilational residual stresses.

6. Concluding remarks

The fact that only few direct observations have been made of a PV as the nucleus of a radial crack, does not imply that this situation is rare. Because transverse fracture is generally initiated at the outer edge of a radial crack, no correlation between the final fracture plane and the initial PV can be expected. Consequently, fracture surface pairs exhibiting the PV–radial crack combination are rare. Nevertheless such examples are occassionally found, as demonstrated by Fig. 9. Furthermore, the average, axial extension of the radial crack being at least an order of magnitude larger than that of a PV, polished sections will display the combination showed by Fig. 5. only incidentally.

It may also be noted that radial cracks often were observed to coincide with core surface notches in earlier reports [2, 6]. These investigations were, however, performed before the nature and importance of PVs was known, and no attention was paid to achieving extreme resolution in these particular areas. It is, thus, possible that imaged notches in fact contain PVs, though not resolved.

The present results also provide some evidence that the radial cracks are formed, or at least completed, after the manufacturing process is finished. If a crack were propagating radially already during the mantle growth, i.e. before the final quench and formation of a compressive surface layer, it would reach the external surface and result in a long, axial surface crack, however such cracks are never observed.

It is interesting to note that the present type of investigation, though in principle qualitative like most electron microscope work, provides a means of measuring and locating residual stresses. With respect to experimental difficulties arising from the small dimensions of the specimen, this method is probably not inferior to bulk methods, reported elsewhere [2, 3]. To some extent, these arguments hold also for the measurement of self-diffusion activation energy and surface energy of boron performed with the aid of electron microscopy and reported previously [6, 8].

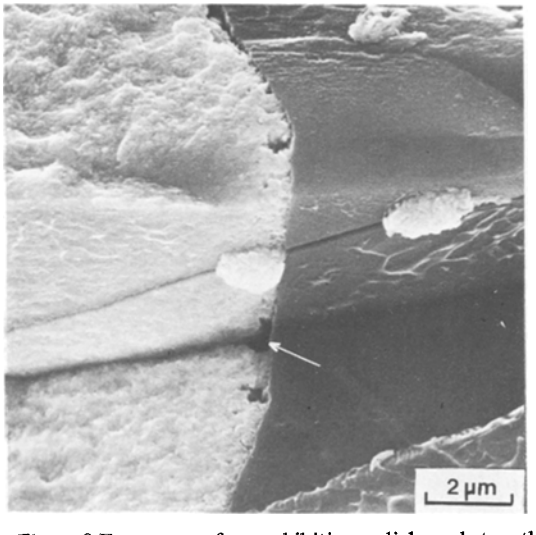

Figure 9 Fracture surface exhibiting radial crack together with a proximate void (arrow) (20 kV SEM).

References

1. C.P. TALLEY, L. LINE and Q. OVERMAN, in "Boron Synthesis, Structure and Properties", edited by I. Kohn, W. Nye and G. Gaulé (Plenum Press, New York, 1960).
2. F.E. WAWNER Jun., in "Modern Composite Materials", edited by L.J. Broutman and R.H. Krock (Addison Wesley, Reading USA, 1967).
3. L.E. LINE Jun. and U.V. HENDERSON Jun., in "Handbook of Fiberglass and Advanced Plastic Composites", edited by G. Lubin (Van Nostrand Reinhold, New York, 1969).
4. R.P.I. ADLER and M.L. HAMMOND, *Appl. Phys. letters*, **14** (1969) 354.
5. J.K. LAYDEN, *J. Mater. Sci.* **8** (1973) 1581.
6. J. VEGA-BOGGIO and O. VINGSBO, *J. Mater. Sci.* **11** (1976) 273.
7. *Idem, J. Mater. Sci.* **11** (1976) 2242.
8. J. VEGA-BOGGIO, J-Å. SCHWEITZ and O. VINGSBO, *J. Mater. Sci.* **12** (1977) 1692.
9. J. VEGA-BOGGIO, J-O. CARLSSON and O. VINGSBO, *J. Mater. Sci.* **12** (1977) 1750.
10. C.P. TALLEY, *J. Appl. Phys.* **30** (1959) 1114.
11. J. VEGA-BOGGIO, J-Å. SCHWEITZ, *J. Mater. Sci.* **12** (1977) 1923.

Received 16 March and accepted 4 April 1977.